Acta Scientiarum

http://periodicos.uem.br/ojs
ISSN on-line: 1807-8664
Doi: 10.4025/actascitechnol.v46i1.69511

Solar Power and Demand Response for Greening Indian Lignite Power Plants: A CO2 Reduction Initiative

Vivek Saxena[1*] and Saurabh Kumar Rajput[2]

[1]Department of Electrical & Computer Engineering, ABES Engineering College, NH-09, Ghaziabad, Uttar Pradesh, 201009, India. [2]Centre for Internet of Things, Madhav Institute of Technology & Research, Gwalior, India. *Author for correspondence E-mail: vvksaxena1234@gmail.com

ABSTRACT. This research paper delves into the prospect of curbing carbon dioxide (CO2) emissions by strategically deploying solar photovoltaic (PV) systems and orchestrating demand response (DR) mechanisms within Indian lignite power plants (LPP). The study responds to the critical imperative of mitigating greenhouse gas (GHG) emissions originating from coal-based electricity generation, a matter of substantial consequence in the context of climate change. In pursuit of optimal solar PV system allocation, this research employs the particle swarm optimization (PSO) technique, considering a spectrum of factors including solar resource availability, electricity demand patterns, and the CO2 intensity associated with coal power generation. The primary objective is to minimize CO2 emissions while maximizing the integration of solar PV and curtailing power losses, all while accounting for the intermittent nature of solar power and the dynamic nature of demand. The proposed approach is rigorously tested on the IEEE 33 bus system, supplied by the LPP. The results convincingly demonstrate a remarkable reduction in CO2 emissions, amounting to 29.69%, following the implementation of the proposed approach. This research presents a concrete step towards a more sustainable and environmentally friendly energy landscape, offering valuable insights for policymakers and stakeholders in the energy sector.

Keywords: Distributed generation; fossil fuel; power quality; PSO; renewable energy.

Received on July 06, 2023.
Accepted on January 10, 2024.

Introduction

Electricity is the lifeblood of modern society, underpinning industrial processes, construction activities, and our day-to-day routines. Yet, the heart of electricity generation predominantly relies on a mix of energy sources, including coal, natural gas, uranium, solar, wind, and hydropower. This indispensable process of power generation bears a heavy environmental burden, chiefly manifested through its pivotal role in global CO2 emissions. Thus, the pivotal choice of generation technology becomes a linchpin in our efforts to mitigate the environmental repercussions of energy production. Notably, renewable energy sources, in stark contrast to coal, stand as a beacon of sustainability, emitting a carbon footprint nearly 20 times smaller (Saxena, Kumar, & Nangia, 2024). According to the Central Electricity Authority's 2022 CO2 baseline database for the Indian power sector (Autoridade Central de Eletricidade [CEA], 2023), LPP emit a substantial 0.975 tons of CO2 per megawatt-hour (tCO2/MWh). The strategic deployment of renewable DG within the Distribution Network (DN) offers a ray of hope to diminish these emissions. However, it's essential to acknowledge that while solar PV systems are a key player in this transformation, their construction relies on electricity from thermal power plants, resulting in a limited carbon footprint. For instance, PV module production incurs a lifetime CO2 emission of approximately 0.053 kg per kWh of electrical energy (Rajput, & Dheer, 2022). The dynamics of India's energy landscape are painted vividly in Figure 1, tracing capacity additions from fiscal year 2000-01 to 2021-22. Notably, coal-based capacity soared from 2000-01 to 2015-16, followed by a significant drop from 2016-17 to 2021-22. In parallel, hydro-based capacity waned from 2017-18 onwards, with other generation capacities showing little activity. This narrative continues in Figure 2, displaying the trend in the weighted average emission factor from fiscal year 2017-18 to 2021-22. Despite a slight uptick in 2021-22 due to increased coal-based generation, gas and hydro-based generation dipped, while the proportion of imported coal decreased from 9% to 4% compared to the preceding fiscal year.

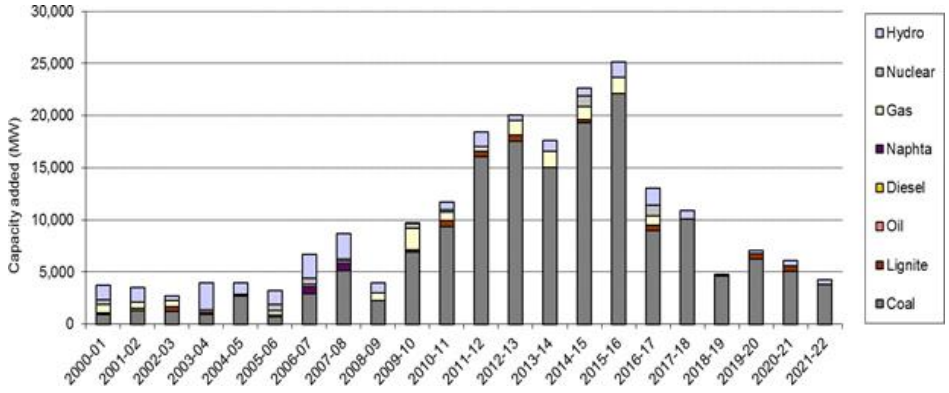

Figure 1. Breakdown of new added capacity covered by the database over the period 2000-01 to 2021-22 (CEA, 2023).

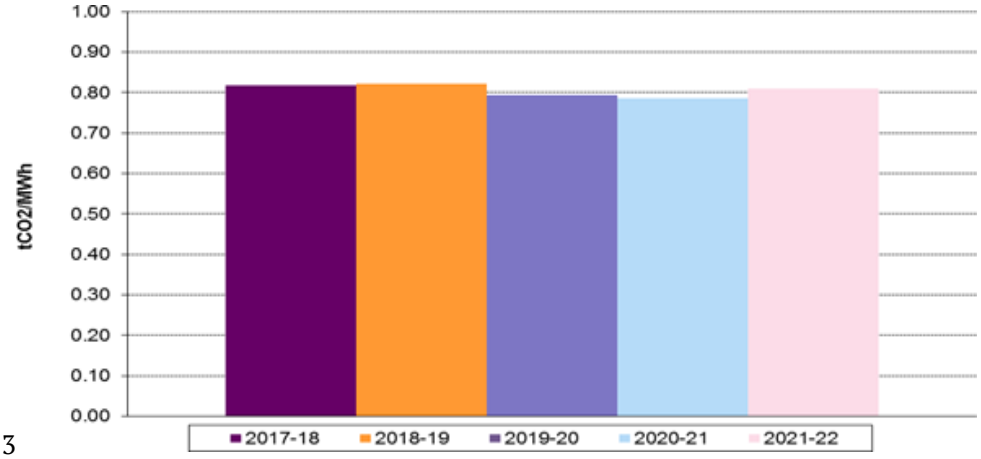

3

Figure 2. Development of the weighted average emission factor for the Indian Grid over the period 2017-18 to 2021-22 (CEA, 2023).

In the realm of energy transformation, DG and DR take center stage in realizing the vision of a smarter grid. DG bifurcates into renewable and non-renewable sources. Renewable DG harnesses naturally replenished resources like solar, wind, hydro, and biomass, offering a sustainable alternative. Non-renewable DG, on the other hand, relies on finite fossil fuel reserves, including diesel generators, natural gas turbines, and fuel cells. This distinction serves as a compass, guiding us towards sustainable energy choices. The optimal placement of solar PV systems within the DN hinges on diverse factors, including load locations, solar resource availability, and DN capacity. The interplay between DR and solar PV's optimal placement has become a focal point of research. DR empowers consumers to adjust electricity consumption in response to price signals, thereby reducing peak demand, enhancing grid reliability, and curbing infrastructure costs (Saxena, Kumar, & Nangia, 2021[a]). Numerous methodologies now dissect how DR influences the optimal placement of solar PV systems. By amalgamating DR and solar PV into the smart grid, we unlock the potential for optimized placements, superior grid performance, and reduced stress on infrastructure. The symbiosis between DR and solar PV represents a critical frontier in forging a more sustainable and efficient energy ecosystem. This research examines several facets of this synergy:

- Capacity Planning: DR's capacity reduction potential influences solar PV placement, as lower capacity requirements may reshape optimal locations.
- Load Profile: The integration of DR can reshape load profiles, potentially altering solar PV placement in response to shifting peak loads.
- Voltage Stability: Solar PV's impact on voltage stability is managed by DR through consumption adjustments, potentially changing optimal placement.
- DN Configuration: DR can alter DN configurations by reducing infrastructure needs or shifting load locations, thus impacting solar PV placement.

Considering these factors in tandem, alongside the integration of DR, we can harness renewable energy resources and infrastructure more efficiently, forging a more sustainable and resilient power system. Research by Zeng, Zhang, Yang, Wang, Dong, and Zhang, (2014) showcases an integrated technique combining renewable distributed generation (RDG) and DR to plan low-carbon, sustainable distribution systems. Their methodology demonstrates substantial benefits over conventional approaches, enhancing RDG efficiency and reducing the DN's

CO2 footprint. Pathiravasam and Venayagamoorthy, (2022) delve into temperature-controlled loads (TCL) within a DR framework, enhancing power system reliability and affordability, especially when coupled with solar power generation. Their study offers insights into optimizing DR for peak reduction and capacity firming, balancing DR reliability and consumer comfort. Liu, Yu, Gao, Lou, and Zhang, (2016) present a framework for a solar PV-based microgrid (PV-MG) and explore DR's impact on its optimization. Their model efficiently minimizes operating costs while adhering to constraints, generating Pareto solutions for diverse scenarios. Zhang, Xu, Dong, and Wong, (2018) propose a robust microgrid coordination strategy, integrating price-based demand response (PBDR) and dispatchable DG to tackle uncertainty. Their robust optimization model ensures economic benefits and efficient management of renewables and demand. Viana, Manassero, and Udaeta, (2018) advocate for regulatory changes to stimulate DR and photovoltaic distributed generation (PVDG). They underscore the importance of economically efficient electricity use, offering a framework for power companies to align with customer energy requirements. Erdinc, Paterakis, Pappi, Bakirtzis, and Catalão, (2015) introduce a comprehensive method that incorporates DR into the sizing of solar PV and energy storage systems, aiming to minimize system costs while ensuring consumer needs are met. Traditional transmission expansion planning (TEP) approaches, as discussed by Hejeejo and Qiu, (2017), based on peak demand, are being challenged by the inclusion of DR and DG. These adaptable approaches enhance power system controllability and cost-effectiveness, adapting to changing demand patterns. As the energy sector accounts for 70% of GHG emissions, especially from coal, distribution companies must pivot towards low-emission coefficient DG units to reduce coal reliance and GHG emissions. Hence, robust computational algorithms are imperative for optimal DG deployment in active distribution systems with a focus on emissions reduction (Lakshmi, Jayalaxmi, & Veeramsetty, 2023).

Material and methods

Problem statement

In the face of escalating energy demand, reducing CO2 emissions by expanding the role of renewable energy sources and minimizing energy losses is imperative. A substantial reduction in CO2 emissions can be achieved by diminishing the reliance on electricity generated by conventional power plants (CPP) and integrating cleaner energy sources. This paper is motivated by the following objectives:

- Minimizing Transmission Losses: Effective power system operation hinges on minimizing transmission losses in the distribution network. These losses result from the inherent resistance in transmission wires, causing voltage drops and energy dissipation during electricity transmission. Thus, the minimization of power loss serves as a primary objective. The loss minimization is mathematically expressed as (Meena, Parashar, Swarnkar, Gupta, & Niazi, 2018):

$$£_1 = \sum_{t=1}^{24} P_{\mathrm{L}\,(t)} \tag{1}$$

$$P_{\mathrm{L}\,(t)} = \sum_{i=1}^{N} \sum_{j=1}^{N} \alpha_{ij\,(t)}\left(P_{i\,(t)}P_{J\,(t)} + Q_{i\,(t)}Q_{J\,(t)}\right) + \beta_{ij\,(t)}\left(Q_{i\,(t)}P_{j\,(t)} - P_{i\,(t)}Q_{j\,(t)}\right) \qquad \forall t \tag{2}$$

where $\alpha_{ij\,(t)} = r_{ij}\cos\left(\delta_{i\,(t)} - \delta_{j\,(t)}\right)/V_{i\,(t)}V_{j\,(t)}$ and $\beta_{ij\,(t)} = r_{ij}\sin\left(\delta_{i\,(t)} - \delta_{j\,(t)}\right)/V_{i\,(t)}V_{J\,(t)}$

- Managing Reverse Power Flow: Reverse power flow occurs when Distributed Generation (DG) units generate more power than local loads require, potentially leading to voltage fluctuations and equipment damage. Careful management and mitigation of reverse power flow are vital objectives. Reverse power flow is defined as:

$$£_2 = \sum_{t=1}^{24} P_{R\,(t)} \tag{3}$$

$$P_{R\,(t)} = \begin{cases} 0, & \text{if } I_{\mathrm{G}\,(t)} \geq I_{\mathrm{S}} \\ \mathrm{Re}\left(V_{\mathrm{G}\,(t)}\, I^{*}_{\mathrm{G}\,(t)}\right) & \text{if } I_{\mathrm{G}\,(t)} < I_{\mathrm{S}}. \end{cases} \tag{4}$$

- Voltage Deviation Management: Voltage deviations from standard levels can result in inefficiencies, increased losses, and equipment damage. The objective is to minimize voltage deviations, expressed as (Safdarian, Degefa, Lehtonen, & Fotuhi-Firuzabad, 2014):

$$£_3 = \left(1 + \sum_{t=1}^{24} V_{D\,(t)}\right) \tag{5}$$

$$V_{D\,(t)} = \begin{cases} \left|V_{\mathrm{Min}} - V_{i\,(t)}\right| & \text{if } V_{i\,(t)} < V_{\mathrm{Min.}} \\ 0 & \text{if } V_{\mathrm{Min.}} \leq V_{i\,(t)} \leq V_{\mathrm{Max.}} \\ \ell & \text{if } V_{i(t)} > V_{\mathrm{Max.}} \end{cases} \tag{6}$$

where ℓ is the large value or unacceptable value.

Fitness function

The optimization combines these objectives into a fitness function with distinct weightage factors for each objective:

$$min(\Upsilon_1) = \varphi \times M \times £_3 \quad (7)$$

where $M = £_1 + £_2$ and φ is the daily to yearly conversion product.

The DR planning and scheduling approach of DGs is taken into consideration at level 2 of the optimization objectives. The following objective function will be taken into consideration for level 2 of the optimization problem:

$$min(\Upsilon_2) = M \times £_3 \quad (8)$$

In this context, the fitness function for level 2 is denoted by Υ_2.

It is vital to have a dispatch strategy, which is determined upon by the DR aggregator. This helps to minimize the aforementioned fitness function.

Demand response aggregator

To address peak demand efficiently, a Demand Response Aggregator (DRA) plays a pivotal role. It collaborates with energy consumers to curtail energy usage during peak periods and subsequently sells the saved energy back to grid operators. DRAs use various technologies and strategies to achieve this, including automated demand response systems and smart thermostats. The paper considers DRAs to optimize the DR process, contributing to grid management, cost mitigation, and system reliability. Restrictions related to DR are carefully managed, ensuring that contracted load and DR penetration rate are upheld. This multi-objective optimization framework aims to minimize losses, manage reverse power flow, and maintain voltage stability while enhancing the integration of renewable energy sources. It incorporates the crucial role of DRAs in this process, ensuring a balanced and sustainable power system (Saxena, Kumar, & Nangia, 2021[b]). DRAs assume a pivotal role in aiding grid operators to proficiently handle peak demand, reduce energy expenses, and bolster system dependability. By providing incentives to energy consumers to curtail their energy consumption during peak periods, DRAs play a key role in equilibrium between electricity supply and demand, thus diminishing the necessity for supplementary generation capacity. Subsequent factors delineate the constraints linked with Demand Response (DR) that are thoughtfully evaluated:

$$P_{i(t)} = \left(P_{Gi(t)} - P_{Di(t)}\right) \qquad \forall t, i \quad (9)$$

$$Q_{i(t)} = \left(Q_{Gi(t)} - Q_{Di(t)}\right) \qquad \forall t, i \quad (10)$$

$$P_{Di(t)} = \left(P_{in,i(t)} + P_{el,i(t)}\right) \qquad \forall t, i \quad (11)$$

$$\sum_{i=1}^{N} \sum_{t=1}^{24} \left(P_{in,i(t)} + P_{el,i(t)}\right) \times \Delta t = E_i^{Total} \quad (12)$$

$$P_{el,i}^{min} \leq P_{el,i(t)} \leq min\left(\left(C - P_{in,i(t)}\right), P_{el,i}^{max}\right) \forall t \quad (13)$$

$$P_{el,i}^{max} = \mu \sum_{t=1}^{24} L_{d,i(t)} \quad (14)$$

where C and μ is the contract load and DR penetration rate respectively.

Objective constraints

The objective functions are subject to a range of constraints, encompassing both technical and operational considerations. These constraints can be expressed numerically as follows:

Solar PV Output Constraint:

$$0 \leq P_{\mathrm{DG},i} \leq P_{DG}^{max} \qquad \forall i \quad (15)$$

Feeder Constraint:

$$I_{ij(t)} \leq I_{ij}^{max} \qquad \forall t, i, j \quad (16)$$

Power Balance Constraints The constraints for real power and reactive power:

$$P_{i(t)} = V_{i(t)} \sum_{j=1}^{N} V_{j(t)} Y_{ij} \cos\left(\theta_{ij} + \delta_{j(t)} - \delta_{i(t)}\right) \qquad \forall t, i \tag{17}$$

$$Q_{i(t)} = -V_{i(t)} \sum_{j=1}^{N} V_{j(t)} Y_{ij} \sin\left(\theta_{ij} + \delta_{j(t)} - \delta_{i(t)}\right) \qquad \forall t, i \tag{18}$$

Modeling of demand

The demand modeling of the system is given in the following equations:

$$P_{D,i(t)} = \Omega_{i(t)} P_{D,i}^{0} \qquad \forall t, i \tag{19}$$

$$Q_{D,i(t)} = \Omega_{i(t)} Q_{D,i}^{0} \qquad \forall t, i \tag{20}$$

where $\Omega_{i(t)}$ is the assigned load factor for the time period t.

Modeling of solar PV output

Solar power generation relies on various additional factors. These factors encompass the characteristics of the solar panel, such as its type and surface area, the tilt angle at which it is positioned, and the level of solar radiation it receives. For the purpose of analysis, it is assumed that all other variables remain constant during the specified period. The calculation for the conversion of current relative to the rated voltage is as follows:

$$I_{sm(t)} = \begin{cases} I_{sm} \text{ if } S_{r(t)} \geq S_r^r \\ I_{sm} \times S_{r(t)} / S_r^r \text{ if } S_{r(t)} < S_r^r \end{cases} \tag{21}$$

Optimization Technique

Particle Swarm Optimization (PSO) is a computational algorithm inspired by the behavior of animals, enabling computers to discover optimal solutions. In this approach, each "particle" symbolizes a potential solution, and these particles adjust their positions and velocities based on collective knowledge. The movement of these particles is directed by the objective function, which steers their search for optimal answers. PSO continually updates a particle's position using its current position, its best-known position, and the swarm's best-known position. This iterative process persists until a predefined stopping condition is met. PSO is widely employed for multilevel optimization tasks, including DG planning. Details of the simulation parameters for this optimization technique are outlined in Table 1, as per the findings in the reviewed literature (Saxena, Kumar, & Nangia, 2022; Saxena, Kumar, & Nangia, 2023).

Table 1. Simulation parameters of multilevel optimization technique.

Parameters	Level-1	Level-2
Swarm size	20	50
Inertia weight	1	1
Inertia Weight Damping Ratio	0.99	0.99
Personal Learning Coefficient	1.5	1.5
Global Learning Coefficient	2	2
Maximum Number of Iterations	50	50

Test system and parameters

In this study, we employ a multilevel optimization approach to assess the IEEE 33 bus system, as depicted in Figure 3 (Baran and Wu, 1989). Specifically, we consider the Indian LPP as the energy source for the power grid. Our research is centered on a comprehensive exploration and evaluation of the effects of DR technologies, aiming to ascertain the most suitable power transmission strategies under varying conditions and constraints. The primary objective is the enhancement of power distribution efficiency. To carry out this investigation, we leverage MATLAB software, running on a computer equipped with an i3 core processor and 12 gigabytes of random-access memory. These computational tools enable us to implement the proposed optimization methodologies and attain our optimization goals effectively. Furthermore, key parameters including base voltage, nominal active demand, nominal reactive demand, power loss, *Vmin*, *Vmax,* and P_{DG}^{max}, are specified as follows: 12.66 kV, 3715 kW, 2300 kVAr, 202.7 kW, 0.95 per unit, 1.05 per unit, and 2 MW, respectively. These parameters play a pivotal role in our analysis and optimization efforts.

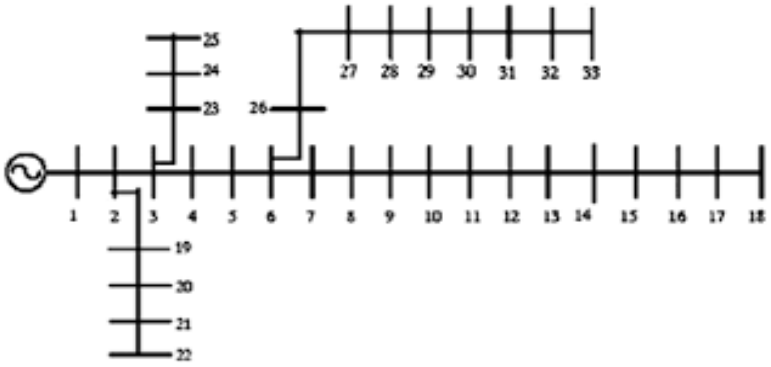

Figure 3. IEEE 33 bus system.

Results and discussion

Base case

In this initial analysis, we consider the baseline scenario to demonstrate the effectiveness of integrating solar PV technology into a 33-bus radial distribution system. Our objective functions are designed based on typical daily consumption patterns, and the annual energy loss is calculated as the average of daily energy losses (Mazidi, Zakariazadeh, Jadid, & Siano, 2014). The lowest demand is observed at approximately 5:00 a.m., with peak demand occurring around 8:00 p.m. As shown in Tables 2, 3, and 4, this base case scenario exhibits disparities for the highest and lowest demand, minimum mean voltage, annual energy losses, and daily CO2 emissions, amounting to 5397.73 kW, 0.978178 per unit, 1426 MWh, and 99047.49 kg, respectively.

Table 2. Effect of the coordination of DR with optimally integrated solar PV on demand.

Case No.	Category	Maximum Demand (kW)	Maximum Demand Mitigation %	Difference between Maximum to Minimum Demand (kW)	% of Maximum Loss Mitigation at 8:00 PM
1	Base Case	6519	0	5397.73	0
2	DG	6519	0	6016.39	0
3	DR@10%	5548	16.1	4166.14	36.09
	DR@20%	5321	18.42	3730.6	42.77
4	DG+DR@10%	5370	17.33	4322.87	33.69
	DG+DR@20%	4790	26.78	3540.31	45.69

Table 3. Outcomes of the coordination of DR with optimally integrated solar PV.

Case No.	Category	Optimal Allocation of DG (Bus No., kW)	Annual Losses (MWh)	Reduced losses / Year (%)	DG Penetration (%)
1	Base Case		1426		
2	DG	17(1344)-32(1690)-25(1092)	1098	23	68.76
3	DR@10%		1302	8.69	
	DR@20%		1290	9.53	
4	DG+DR@10%	7(1086)-15(1902)-32(914)	996	30.15	65.03
	DG+DR@20%	18(408)-29(1816)-11(1602)	934	34.5	63.76

Table 4. Impact of proposed framework on CO2 emission of LPP.

Case	Energy Demand from LPP/Day (kWH)	Energy Supplied from DG/Day (kWh)	CO2 emission from Solar PV (Kg)	Energy Losses / Day (kWh)	Energy Supplied from LPP/Day (kWH)	CO2 emission/Day (Kg) by LPP	Total CO2 emission/Day (Kg)	% Reduction in CO2 emission /Day
Base Case	73474			3906.85	77380.85	99047.49	99047.49	
DG	52681	20793	1102.029	3008.22	55689.22	71282.20	72384.23	26.85%
DR@10%	73472			3567.12	77039.12	98610.08	98610.08	0.30%
DR@20%	73411			3534.25	76945.25	98489.92	98489.92	0.49%
DG+DR@10%	50684	22790	1207.87	2728.77	53412.77	68368.34	69576.21	29.69%
DG+DR@20%	54498	18976	1005.728	2558.90	57056.90	73032.84	74038.57	25.18%

Integration of DG

Here, we delve into an optimization study involving the integration of DGs through solar PV installations in a DN. The results reveal significant enhancements in power quality parameters. Notably, we observe a substantial 21.8% reduction in annual energy loss and an increase in the minimum mean voltage from 0.978178 to 0.99634 per unit. Table 3 provides valuable insights into the optimal sizing and locations of solar PV installations. Additionally, Figures 4, 5, and 6 visually depict the impact of DGs on demand patterns, voltage levels, and active power losses, respectively. This integration of solar PV into the DN leads to a remarkable 26.85% reduction in CO2 emissions.

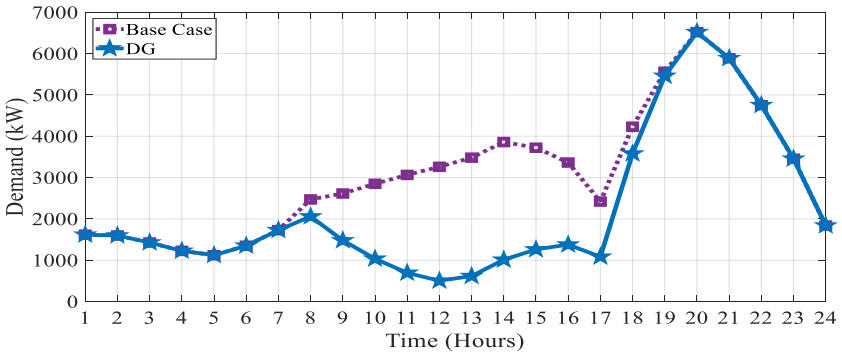

Figure 4. Impact of DG on demand curve.

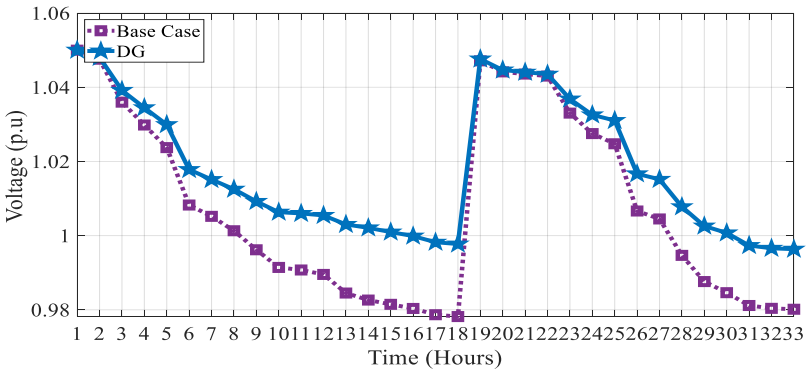

Figure 5. Impact of DG on voltage curve.

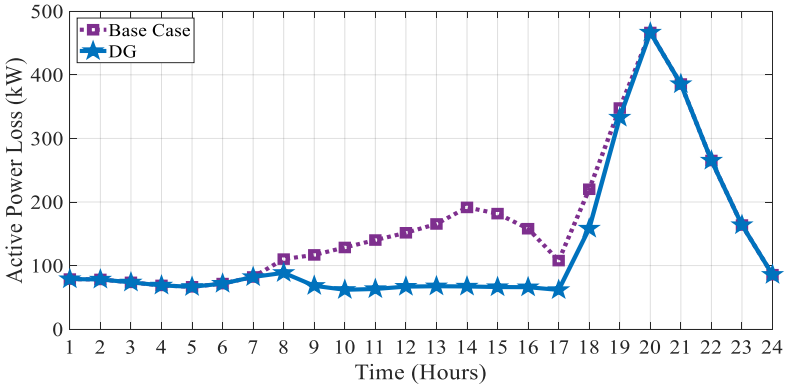

Figure 6. Impact of DG on power losses.

DR approach

In this scenario, we evaluate the significance of the DR approach in the absence of DG coordination. We assume and compare two levels of demand elasticity. DR rates representing market demand elasticity are considered at 10% and 20% without DG placement. The results demonstrate that DR effectively reduces peak demand by 14.72 for a 10% DR rate and 18.32 for a 20% DR rate, along with yearly energy loss reductions ranging from 5.96 to 8.2%. DR also contributes to reductions in active power losses and an increase in peak-to-valley disparity. Remarkably, even without DG, DR proves to be effective.

Figures 7, 8, 9, and 10 provide insights into the effects of 10 and 20% DR rates on demand, voltage, and active power losses. Furthermore, the impact of the DR rate on the voltage profile and CO2 emissions of the test system is found to be negligible.

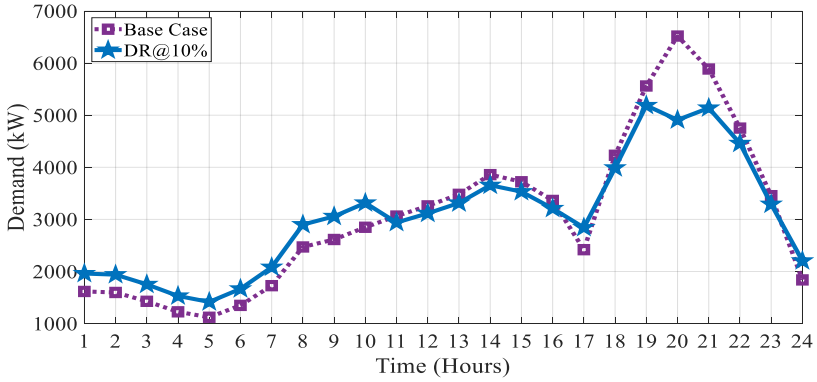

Figure 7. Impact of DR@10% on demand curve.

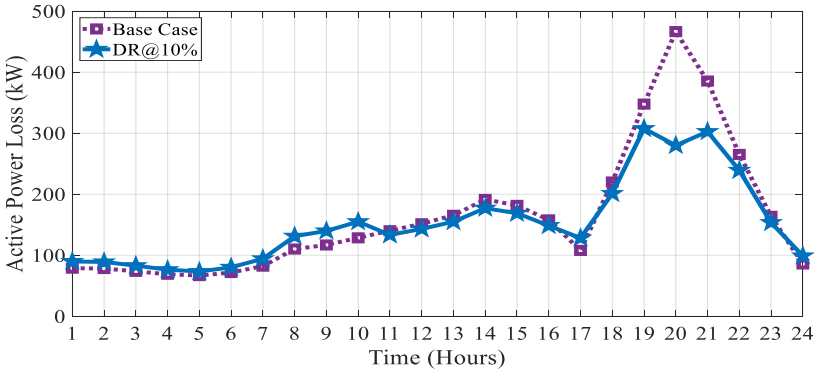

Figure 8. Impact of DR@10% on power losses.

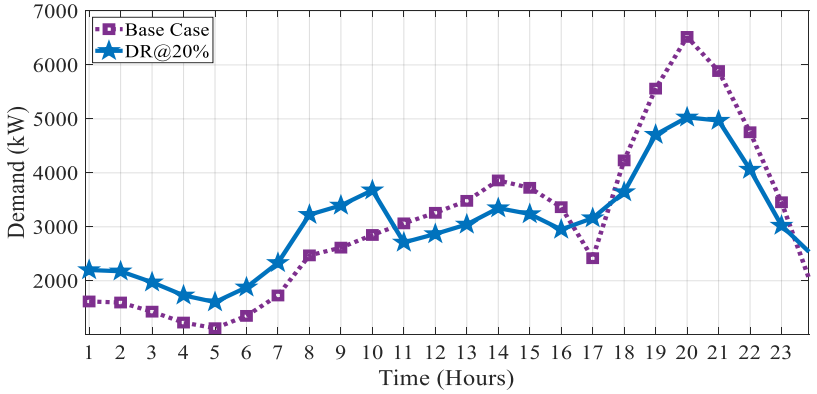

Figure 9. Impact of DR@20% on demand curve.

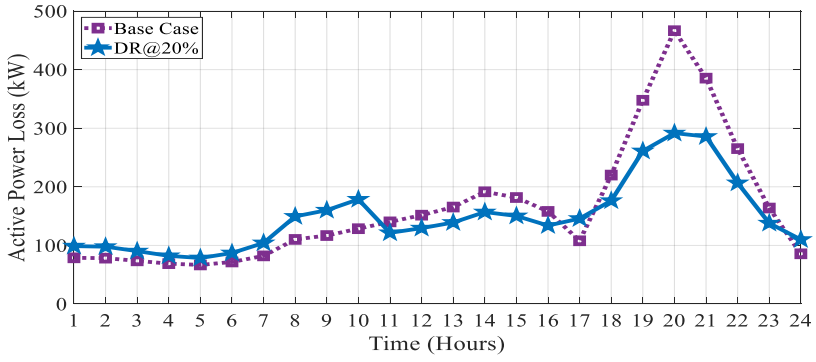

Figure 10. Impact of DR@2.

DG and DR coordination

In this final analysis, we investigate the integration of DGs into DR coordination and planning while considering system constraints. This scenario explores DG integration with DR scheduling under varying DR rates and DG sizes. The results indicate improved system performance, with a substantial reduction in annual energy loss, ranging from 29.03 to 33.31% compared to cases 1 and 2, depending on the DR rates. Additionally, the lowest mean voltage increases significantly with the presence of DGs. The load profile becomes flatter as DGs minimize the gap between maximum and minimum demand. Figures 11, 12, and 13 illustrate the impact of DGs with a 10% DR rate on demand, voltage, and active power losses, while Figures 14, 15, and 16 depict the effect of DGs with a 20% DR rate. Notably, in the presence of DGs, CO2 emissions are reduced by 29.69 and 25.18% for DR rates of 10 and 20%, respectively.

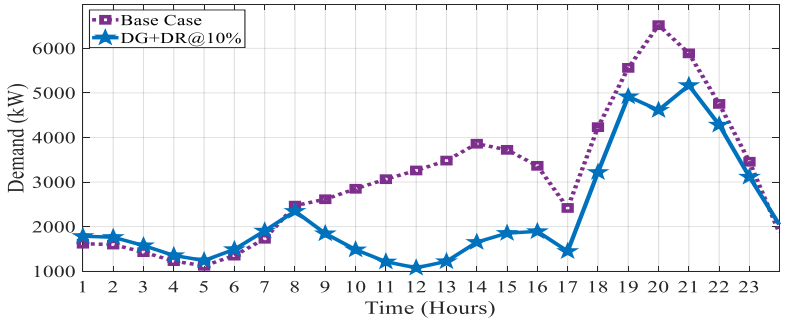

Figure 11. Impact of DG+DR@10% on demand curve 0% on power losses.

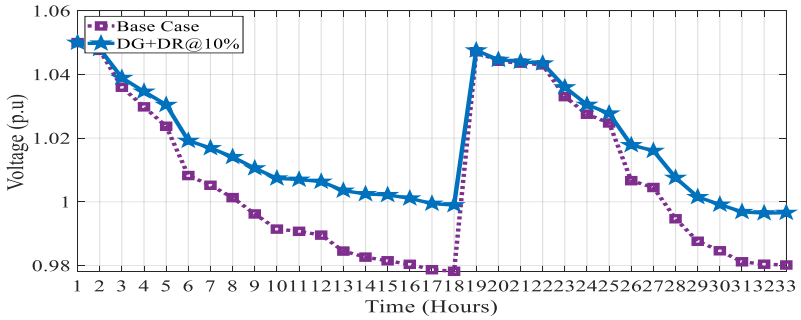

Figure 12. Impact of DG+DR@10% on voltage curve.

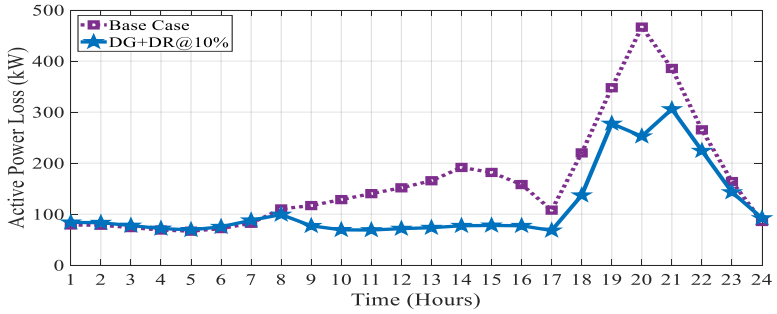

Figure 13. Impact of DG+DR@10% on power losses.

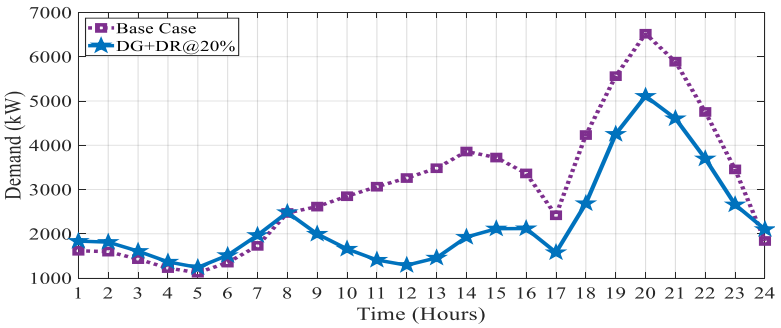

Figure 14. Impact of DG+DR@20% on demand curve.

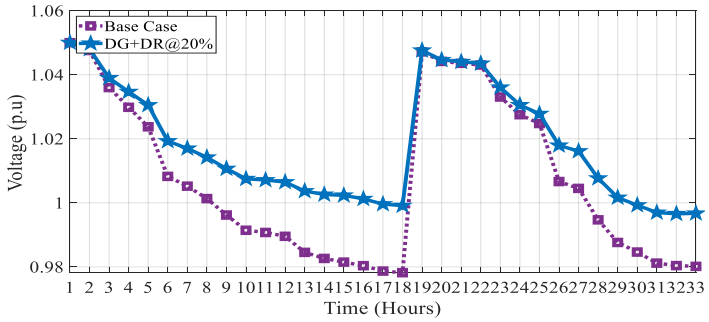

Figure 15. Impact of DG+DR@20% on voltage curve.

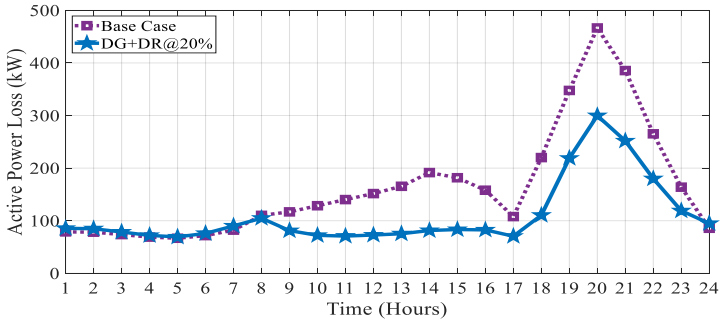

Figure 16. Impact of DG+DR@20% on power losses.

Figure 17 illustrates the total CO2 emissions per day across various scenarios, comparing the emission levels between the base case and the proposed approach. This comparison highlights how the proposed method significantly reduces CO2 emissions, demonstrating its environmental advantages over the base case.

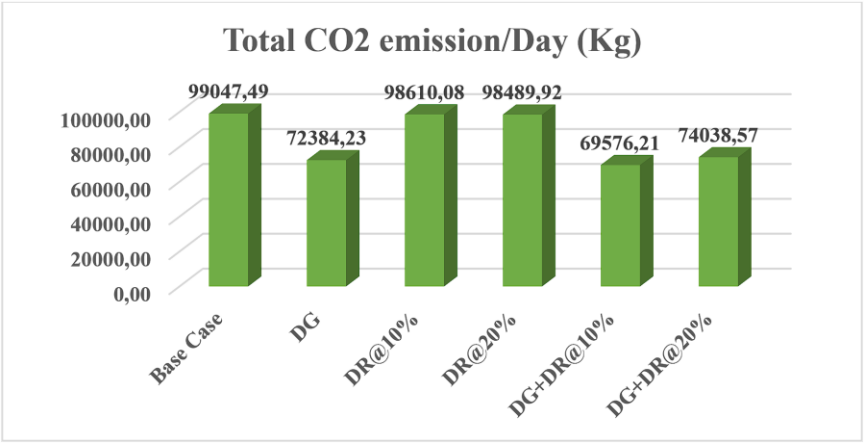

Figure 17. Total CO2 emission per day in different cases.

Abbreviations

$P_{L\,(t)}$	Power transmission losses
$P_{i\,(t)}$	Real power at ith node at any time t
$P_{J\,(t)}$	Real power at jth node at any time t
$Q_{i\,(t)}$	Reactive power at ith node at any time t
$Q_{J\,(t)}$	Reactive power at jth node at any time t
$V_{i\,(t)}$	Voltage at ith node at any time t
$V_{J\,(t)}$	Voltage at jth node at any time t
r_{ij}	Resistance of branch between ith and jth node
$\delta_{i\,(t)}$	Angle of voltage at ith node
$\delta_{j\,(t)}$	Angle of voltage at jth node
$P_{R\,(t)}$	Reverse power at time t

$I_{\mathrm{G}\,(t)}$	Current from grid at time t
$V_{\mathrm{G}\,(t)}$	Voltage of grid at time t
$I_{\mathrm{S.}}$	Designated limit of reverse current
$V_{D\,(t)}$	Penalty for deviation of voltage
$V_{\mathrm{Max.}}$	Maximum value of permissible voltage at node
V_{Min}	Minimum value of permissible voltage at node
$P_{Gi(t)}$	Real power generation at ith node for the time period t
$P_{Di(t)}$	Real power demand for the time period t
$Q_{Gi(t)}$	Reactive power generation at ith node for the time period t
$Q_{Di(t)}$	Reactive power demand for the time period t
$P_{in,i(t)}$	Nonreceptive load at time t
$P_{el,i(t)}$	Receptive load at time t
E_i^{Total}	Energy demand per day
$L_{d,i(t)}$	Load per hour for the time period t
$P_{\mathrm{DG},i}$	Real power injection by DG
P_{DG}^{max}	Maximum value of real power generation by DG
$I_{ij(t)}$	Current flowing between ith and jth Node at t
I_{ij}^{max}	Maximum permissible value of current
Y_{ij}	Admittance matrix between ith and jth Node
θ_{ij}	Angle of impedance between ith and jth Node
I_{sm}	Current of solar PV
$S_{r(t)}$	Solar radiation at t
S_r^r	Rated value of solar radiation for PV

Conclusion

In summary, this research paper addresses a critical issue: the reduction of CO2 emissions in the Indian LPP through the optimization of solar PV system allocation and the coordination of DR. By integrating renewable energy DGs like solar PV, this study offers a promising solution to mitigate greenhouse gas emissions from the coal-based electricity generation sector. This research employs PSO to determine the optimal allocation of solar PV systems, taking into account various factors such as solar resource availability, electricity demand patterns, and the CO2 intensity of coal power generation. The primary objectives are to minimize CO2 emissions, maximize solar PV penetration, and minimize power losses, all while considering the intermittent nature of solar power and dynamic demand. The effectiveness of this approach is demonstrated on the IEEE 33 bus system, which is supplied by an LPP.

The results are striking, revealing a substantial 29.69% reduction in CO2 emissions after implementing the proposed approach. These findings underscore the immense potential and effectiveness of integrating solar PV systems and coordinating demand response to significantly reduce CO2 emissions in the coal-based electricity generation sector, thereby contributing significantly to global efforts to mitigate climate change.

While DGs have proven effective in reducing annual energy losses, it's essential to acknowledge their potential impact on load profile flattening. As DG penetration increases, voltage levels can rise, leading to reverse power flow back into the grid. These challenges underline the limitations of high DG penetration within the DN. However, the incorporation of DR helps balance the load profile, minimize the gap between peak and off-peak load demands, and alleviate strain on the system. In essence, a higher DR rate can enhance demand normalization efficiency, particularly in scenarios where the penetration level of solar PV systems is lower.

According to the implemented framework, the mitigation of maximum demand, reduced annual energy losses, and DG penetration reach impressive levels, reaching 26.78, 34.5, and 67.76%, respectively. These represent the maximum achievements from case 1 to case 4.

In conclusion, it can be deduced that the optimal placement of solar PV systems, coupled with an optimal DR rate, stands as a highly effective strategy for reducing CO2 emissions in the LPP. This approach not only demonstrates a substantial reduction in emissions but also underscores the potential for cleaner and more sustainable energy solutions in the Indian electricity landscape.

References

Baran, M. E., & Wu, F. F. (1989). Network reconfiguration in distribution systems for loss reduction and load balancing. *IEEE Transactions on Power Delivery, 4*(2), 1401-1407. DOI: https://doi.org/10.1109/61.25627

Autoridade Central de Eletricidade [CEA]. (2023). Emission: 2021-22. [Online]. Retrieved from https://cea.nic.in/wpcontent/uploads/baseline/2023/01/Approved_report_emission__2021_22.pdf

Erdinc, O., Paterakis, N. G., Pappi, I. N., Bakirtzis, A. G., & Catalão, J. P. S. (2015). A new perspective for sizing of distributed generation and energy storage for smart households under demand response. *Applied Energy, 143*, 26-37. DOI: https://doi.org/10.1016/j.apenergy.2015.01.025

Hejeejo, R., & Qiu, J. (2017). Probabilistic transmission expansion planning considering distributed generation and demand response programs. *IET Renewable Power Generation, 11*(5), 650-658. DOI: https://doi.org/10.1049/iet-rpg.2016.0725

Lakshmi, G. V. N., Jayalaxmi, A., & Veeramsetty, V. (2023). Optimal placement of distributed generation based on DISCO's financial benefit with loss and emission reduction using hybrid Jaya–Red Deer optimizer. *Electrical Engineering, 105*, 965-977. DOI: https://doi.org/10.1007/s00202-022-01709-y

Liu, S., Yu, W., Gao, W., Lou, K., & Zhang, Y. (2016). Multi-objective optimization dispatch of PV-MG considering demand response actions. *In 2016 35th Chinese Control Conference*. 2728-2733. Chengdu, China. DOI: https://doi.org/10.1109/ChiCC.2016.7553777

Mazidi, M., Zakariazadeh, A., Jadid, S., & Siano, P. (2014). Integrated scheduling of renewable generation and demand response programs in a microgrid. *Energy Conversion and Management, 86*, 1118-1127. DOI: https://doi.org/10.1016/j.enconman.2014.06.078 (have been cited in the text)

Meena, N. K., Parashar, S., Swarnkar, A., Gupta, N., & Niazi, K. R. (2018). Improved elephant herding optimization for multiobjective DER accommodation in distribution systems. *in IEEE Transactions on Industrial Informatics, 14*(3), 1029-1039. DOI: https://doi.org/10.1109/TII.2017.2748220

Pathiravasam, C., & Venayagamoorthy, G. K. (2022). Distributed demand response management for a virtually connected community with solar power. *IEEE Access, 10*, 8350-8362. DOI: https://doi.org/10.1109/ACCESS.2022.3141772

Rajput, S. K., & Dheer, D. K. (2022). Integration of 100-kWp PV with low-voltage distribution power system in composite climate: performance and energy metrics analysis. *International Journal of Ambient Energy, 43*(1), 8176-92. DOI: https://doi.org/10.1080/01430750.2022.2092775

Safdarian, A., Degefa, M. Z., Lehtonen, M., & Fotuhi-Firuzabad, M. (2014). Distribution network reliability improvements in presence of demand response. *IET Generation, Transmission & Distribution, 8*(12), 2027-2203. DOI: https://doi.org/10.1049/iet-gtd.2013.0815

Saxena, V., Kumar, N., & Nangia, U. (2021a). Smart grid: A sustainable smart approach. *Journal of Physics: Conference Series, 1*, 012042. DOI: https://doi.org/ 10.1088/1742-6596/2007/1/012042

Saxena, V., Kumar, N., & Nangia, U. (2022). an impact assessment of distributed generation in distribution network. *Artificial Intelligence and Sustainable Computing.* 33-46. DOI: https://doi.org/10.1007/978-981-19-1653-3_26

Saxena, V., Kumar, N., & Nangia, U. (2021b). Analysis of smart electricity grid framework unified with renewably distributed generation. *Advances in Smart Communication and Imaging Systems. Lecture Notes in Electrical Engineering, 721*, 735-751. DOI: http://dx.doi.org/10.1007/978-981-15-9938-5_68

Saxena, V., Kumar, N., & Nangia, U. (2023). An extensive data-based assessment of optimization techniques for distributed generation allocation: conventional to modern. *Archives of Computational Methods in Engineering, 30*, 675-701. DOI: https://doi.org/10.1007/s11831-022-09812-w

Saxena, V., Kumar, N., & Nangia, U. (2024). Computation and optimization of BESS in the Modeling of Renewable Energy Based Framework. *Archives of Computational Methods in Engineering, 31*, 2385-2416. DOI: https://doi.org/10.1007/s11831-023-10046-7

Viana, M. S., Manassero, G., & Udaeta, M. E. M. (2018). Analysis of demand response and photovoltaic distributed generation as resources for power utility planning. *Applied Energy, 217*, 456-466. DOI: https://doi.org/10.1016/j.apenergy.2018.02.153

Zhang, C., Xu, Y., Dong, Z. Y., & Wong, K. P. (2018). Robust coordination of distributed generation and price-based demand response in microgrids. *IEEE Transactions on Smart Grid, 9*(5), 4236-4247. DOI: https://doi.org/110.1109/TSG.2017.2653198

Zeng, B., Zhang, J., Yang, X., Wang, J., Dong, J., & Zhang, Y. (2014). Integrated planning for transition to low-carbon distribution system with renewable energy generation and demand response. *IEEE Transactions on Power Systems, 29*(3), 1153-1165. DOI: https://doi.org/10.1109/TPWRS.2013.2291553